Molecular Vision 2023; 29:140-152 <http://www.molvis.org/molvis/v29/140>
Received 20 April 2022 | Accepted 1 August 2023 | Published 17 August 2023

Aqueous humor cytokines are associated with baseline optical coherence tomography imaging features in eyes with diabetic macular edema

Tuan Tran,[1,2,3] Paul Sanfilippo,[2] Jonathon Goh,[2,3] Lyndell L. Lim,[2,3] Sukhpal Sandhu,[2,3] Sanjeewa Wickremasinghe[2,3]

[1]University of Sydney, Save Sight Institute, Sydney NSW, Australia; [2]Centre for Eye Research Australia, Royal Victorian Eye and Ear Hospital, Victoria, Australia; [3]Royal Victorian Eye and Ear Hospital, East Melbourne, Victoria, Australia

Purpose: This study aimed to assess the association between cytokine expression and optical coherence tomography (OCT) features of diabetic macular edema (DME).

Methods: This is a post-hoc analysis of the baseline data of a prospective study designed to evaluate the effect of intravitreal ranibizumab injections on aqueous humor cytokine levels in patients with center-involved DME. OCT images were evaluated for baseline imaging features of DME, including central macular thickness (CMT), macular volume (MV), subretinal fluid (SRF) height, morphological pattern of DME, intraretinal cyst (IRC) size, status of the ellipsoid zone/external limiting membrane (EZ/ELM), presence of disorganization of retinal inner layers (DRIL), number of hyperreflective foci (HRF), and the presence of epiretinal membrane (ERM) or vitreomacular traction (VMT). Hierarchical cluster analysis (HCA) was used to identify two groups (clusters) of subjects that shared similar cytokine characteristics (low and high expression profiles), and differences in OCT imaging parameters across clusters were compared using multivariable logistic regression models.

Results: Aqueous cytokine concentrations and OCT images were obtained from 30 eyes of 25 patients recruited. The HCA demonstrated that eyes in the low-concentration cytokine profile group were associated with better BCVA (OR = 0.90, [95% CI 0.81–0.99], p = 0.05), thinner CMT (OR = 1.08, [95% CI 1.01–1.17], p = 0.03), and lower MV (OR = 2.08, [95% CI 1.10–3.90], p = 0.02). Reduced BCVA, greater CMT, and larger MV were individually correlated with multiple cytokines, including IL-7, IL-9, MIP-1α, and TNF-α. Increased SRF was significantly associated with IL-15 (r = 0.40, p = 0.03) and eotaxin (r = 0.47, p = 0.008). Increased levels of IL-6 (H = 39, p = 0.04), IL-13 (H = 44, p = 0.02), and sVEGFR-1 (H = 25.5, p = 0.05) were associated with the presence of DRIL, whereas GM-CSF was protective (H = 131, p = 0.01).

Conclusions: These findings associate higher cytokine expression with worse BCVA, CMT, and MV. Although it is likely that multiple cytokines are associated with the functional and anatomic features of DME, we identified specific cytokines that may drive the process, such as TNF-α, IL-6, IL-7, and IL-9.

Diabetic retinopathy is the leading cause of blindness among working-aged adults with diabetic macular edema (DME), the most common vision-impairing complication. DME is caused by changes in the retinal microvasculature encompassing endothelial cell dysfunction, capillary basement membrane thickening, and a reduced number of pericytes. The resulting vascular permeability and leakage cause fluid accumulation manifested as DME, culminating in retinal dysfunction and vision impairment [1].

There is growing emphasis on the role of inflammation and immune dysregulation in the pathophysiology of DME. Metabolic and oxidative stress from chronic hyperglycemia induces leukostasis and inflammatory breakdown of the blood–retina barrier driven by the coordination of cytokines and growth factors further promoting inflammation [2]. Elevated inflammatory cytokines, such as TNF-α, IL-1β, IL-6 and MCP-1, have been regularly associated with the severity of DME [3-6]. In the DISCERN study [7], we demonstrated changes in the concentrations of multiple cytokines after treatment with intravitreal ranibizumab (IL-1β, IL-7, IL-8, IL-10, IL-12, IL-17, MCP-1, and TNF-α). More recent studies have associated various aqueous cytokines with visual or anatomic responses to treatment with anti-VEGF agents [8-10].

Anti-VEGF-resistant cases of DME classified by worsening or lack of improvement in central macular thickness (CMT) or best-corrected visual acuity (BCVA) can be seen in up to 32%–66% of patients, despite intensive treatment regimes [11-13]. The underlying mechanisms by which these

Correspondence to: Sanjeewa Wickremasinghe, Centre for Eye Research Australia, Level 1, St Andrews Place, East Melbourne. VIC 3002, Australia; Phone: +61 (03) 9929 8360 email: swi@unimelb.edu.au

cases differ in their response to anti-VEGF agents is still unclear; however, alternative treatments, such as intravitreal corticosteroids, have proven effective in providing anatomic and functional improvement in such cases [14,15], thereby implicating a significant role of inflammation in DME. Furthermore, intravitreal dexamethasone and triamcinolone have been shown to improve DME by not only reducing VEGF levels but also by targeting the synthesis of proinflammatory mediators involved in DME, such as IL-6, IL-8, MCP-1, ICAM-1, TNF-α, VEGF, and Ang 2 [16-18].

A wide range of phenotypic manifestations of DME are considered imaging biomarkers that may predict treatment response and outcomes. Such OCT features include central macular thickness (CMT), macular volume (MV), subretinal fluid (SRF), morphological patterns, size of intraretinal cysts (IRC), hyper-reflective foci (HRF), disruption of the ellipsoid zone or external limiting membrane, disorganization of retinal inner layers (DRIL), and presence of epiretinal membrane (ERM) [19]. Recent studies have suggested that certain imaging biomarkers may be associated with raised aqueous or vitreous cytokine levels, and thus be contributed by inflammatory components involved in the pathophysiology of DME [20,21]. Analyzing inflammatory cytokines and potential links to imaging biomarkers may improve our understanding of the mechanisms of DME and support individualized therapeutic decision making. The objective of this study was to investigate the association of intraocular cytokines with the imaging features of eyes with DME.

METHODS

This study was approved by the Human Research and Ethics Committee of the Royal Victorian Eye and Ear Hospital, Melbourne, Australia as part of the DISCERN (Diabetic macular edema: aqueous and Serum Cytokine profiling to determine the Efficacy of RaNibizumab) study and registered with the Australian New Zealand Clinical Trial Registry (ANZCTR identification number 12615000830594). The research adhered to the tenets of the Declaration of Helsinki, and written informed consent was obtained from all participants before enrollment in the study.

This post hoc analysis is based on the cohort of patients enrolled in the DISCERN study. A detailed description of the study design, patient treatment schedule, and aqueous sampling and analysis has been published [7], but in brief, patients with center-involved DME were recruited from the medical retina clinics at the Royal Victorian Eye and Ear Hospital, Melbourne, Australia, between September 2015 and May 2016. All recruited patients had eyes with DME affecting the foveal center and best-corrected visual acuity (BCVA) of 17–72 logarithms of the minimum angle of resolution (LogMAR) letters (Snellen equivalent, 20/400 to 20/40). Although the DISCERN study's treatment schedule involved treating patients with intravitreal ranibizumab from baseline up to 48 weeks, as per the RESTORE protocol [22], this study only assessed baseline cytokine measurements with baseline OCT characteristics.

Aqueous sampling and processing: Aqueous humor samples (0.05–0.1 ml) were obtained from all patients immediately before intravitreal treatment with ranibizumab. Undiluted samples underwent multiplex immunoassay based on Luminex xMAP technology, and the levels of 32 different cytokines were measured using multiplex detection kits from Bio-Rad (Hercules, CA) and Millipore (Billerica, MA). These cytokines included IL-1b, IL-1ra, IL-2, IL-4, IL-5, IL-6, IL-7, IL-8, IL-9, IL-10, IL-12, IL-13, IL-15, IL-17, eotaxin, granulocyte colony-stimulating factor (G-CSF), granulocyte-macrophage CSF (GM-CSF), monocyte chemoattractant protein-1 (MCP-1), platelet-derived growth factor subunit B, TNF-α, epidermal growth factor (EGF), erythropoietin (EPO), IFN-c, basic FGF (FGF-β), IFN-c-induced protein 10 (IP-10), macrophage inflammatory protein (MIP)-1α, MIP-1β, angopoietin-2 (Ang-2), regulated on activation, normal T-cell expressed and secreted (RANTES), VEGF, soluble VEGF receptor-1 (sVEGFR-1), and soluble VEGF receptor 2 (sVEGFR-2). Standard curves were generated with the reference cytokine sample supplied in the kit using the Bio-Plex200 System (software version 5.1.1; Bio-Rad Laboratories) and were used to calculate the cytokine concentrations (pg/mL) of aqueous humor samples. Each cytokine had a different standard curve and a lower limit of detection on the standard curve of cytokine concentration. Cytokine levels that were below the lower limits of detection were recoded, assigned a numerical value of 0 pg/ml, and included in statistical analysis. We were unable to detect IL-2, RANTES, EPO, and Ang-2 in any sample; therefore, they were excluded from further analysis.

Standardized image acquisition and evaluation: Spectral domain optical coherence tomography (OCT) scans were obtained at each patient visit using Heidelberg Spectralis (Heidelberg Engineering, Heidelberg, Germany). A trained masked grader ensured that all scans were adequately centered on the fovea and were re-centered if necessary. For quantitative and qualitative analysis of OCT images, 49 high-resolution horizontal raster B-scans (spanning 20° × 20° [5.7 mm × 5.7 mm]) centered on the fovea with 120 µm distance between each scan.

The foveal centered SD-OCT scans provided quantitative measurements of the central macular thickness (CMT) and macular volume (MV) within the Early Treatment Diabetic

Retinopathy Study (ETDRS), defined as a central zone of 500 µm radius. The Spectralis® software automatically obtained measurements by the in-built "thickness map" function.

For assessing the qualitative features of DME, the horizontal area considered was outlined by the width of horizontal scans (11.4 mm), while the vertical area assessed included five scans above and below the central horizontal scan through the foveola (12 mm height). Each scan was graded by two independent masked retinal specialists (TT and JG), and discrepancies were adjudicated by a third grader (SW).

The morphological pattern of DME was graded as either (1) diffuse retinal thickening (DRT), (2) cystoid macular edema (CME), or (3) serous retinal detachment (SRD), as previously defined by other studies [23,24]. Intraretinal cyst (IRC) size was graded as absent, small, intermediate, or large with the use of reference figures [19], as defined elsewhere [24,25]. The status of the ellipsoid zone (EZ) and the external limiting membrane (ELM) were evaluated within a 1-mm area of the central fovea and graded as either intact or disrupted, as previously defined [19,23,26].

Disorganization of the inner retinal layers (DRIL) was graded as either absent or present [27]. Hyper-reflective foci (HRF) were defined as discrete well circumscribed dots of equal or higher reflectivity than the RPE band. The inclusion and exclusion criteria of HRF were analyzed as defined by Vujosevic et al. [28] HRF were manually counted within the central square area (11.4 × 12 mm) and were graded as follows: '0' = none, '1' = 1–20 and '2' ≥21. Scans were graded as either having the presence or absence of either vitreomacular traction (VMT) or epiretinal membrane (ERM), as described elsewhere [29].

Statistical analysis: BCVA, CMT, MV, and SRF were measured as continuous variables. pattern of IRC, EZ/ELM integrity, HRF, DRIL, and the presence of ERM/ VMT were considered as categorical variables. For the continuous variables (BCVA, CMT, MV, SRF), Spearman correlation was estimated for each variable with the corresponding individual cytokine, and the results are graphed as scatter plots with a loess curve fitted. For categorical variables (pattern, IRC, EZ/ELM, HRF, ERM/VMT, and DRIL), Mann–Whitney (2 levels) or Kruskal–Wallis test (>2 levels) tests were performed, followed by pairwise Wilcoxon tests using the Benjami & Hochberg (false-discovery rate) adjustment for multiple comparisons.

Hierarchical cluster analysis (HCA) was used to identify two groups (clusters) of subjects that shared similar cytokine characteristics (expression profiles). This was a separate analysis in which the goal of HCA was to build a tree diagram of the cytokine expression profiles, with profiles most similar across subjects placed on branches that were close together, thus forming natural clusters. Cytokine values were first rescaled to z-scores by subtracting the mean cytokine value from each subject's recorded measurement and then dividing it by the standard deviation of the particular cytokine. The Euclidean distance metric and Ward's (minimum variance) method were used as the dissimilarity metric and clustering method, respectively. Dendrograms and heatmaps were generated to visualize the clusters and scaled cytokine values. Warmer (more intensely red) colors on the heatmap represent high cytokine values, white colors represent average values, while cooler colors (more intensely blue) represent low values.

Statistical analyses were performed to compare differences in BCVA and OCT imaging parameters (CMT, MV, and SRF) across high or low cytokine expression cluster profiles. Separate multivariable logistic regression models were created with BCVA and each OCT parameter specified (CMT, MV, and SRF) as predictors of each cluster of either high or low expression profiles (adjusted for age and sex). All statistical analyses were conducted in the R statistical environment with HCA performed using the heatmap package (R v4.0.5; R Foundation for Statistical Computing, Vienna, Austria). All tests were two-sided, with a p value <0.05 considered statistically significant.

RESULTS

Characteristics: A total of 30 eyes of 25 patients with center-involving DME were recruited from the DISCERN study [7]. The mean (SD) age at presentation was 63.0 (19.0) years, with a range of 41–82 years, while the mean HbA1c was 7.5% (±1.2). The DR severity according to the ETDRS DRSS ranged from 31 to 81, with 15 eyes (51.7%) being classified as mild to moderate non-proliferative diabetic retinopathy (DRSS score 31–43), 3 eyes (10.3%) were classified as having moderate non-proliferative diabetic retinopathy (DRSS 47), and the remainder had severe non-proliferative diabetic retinopathy or quiescent proliferative DR (12 eyes, 38.0%) and had a DRSS >47.

The mean BCVA was 59.3 letters (± 10.3), mean CMT was 490.6 µm (±134.3), mean MV was 11.2 mm^3 (±2.0) and mean SRF was 45 µm (±71.1). Regarding the morphological pattern of DME, 4 eyes had DRT, 14 had CME, and 12 had SRD at baseline. In total, 4 eyes were considered as having small IRC, whereas 9 were graded as intermediate, and 17 were graded as large. Considering the integrity of the EZ/ELM at baseline, 6 patients had intact EZ/ELM, 19 had disrupted EZ/ELM, and 5 had the structure classified as absent. DRIL was present in 7 eyes, while ERM was present

Table 1. Distribution of values below the lower limit of detection and Median aqueous concentrations (pg/ml) of inflammatory and angiogenic cytokines in eyes diabetic macular edema at baseline (n=30).

Cytokine	Lower limit of detection (pg/ml)	Below detectable range n (%)	Median concentration (pg/ml)	IQR
IL-1β	0.31	8 (26.7)	0.55	0 – 0.77
IL-1RA	5.44	10 (33.3)	25.42	25.42 – 70
IL-4	0.13	0 (0.0)	1.01	0.82 – 1.31
IL-5	0.82	29 (96.7)	0	0
IL-6	1.35	0 (0.0)	73.24	9.73 – 206.59
IL-7	0.64	3 (10.0)	6.82	3.87 – 9.39
IL-8	1.46	0 (0.0)	13.25	7.79 – 25.7
IL-9	0.76	0 (0.0)	7.12	3.12 – 12.1
IL-10	2.62	0 (0.0)	11.56	9.24 – 14.81
IL-12	2.22	0 (0.0)	17.41	12.67 – 24.21
IL-13	0.38	22 (73.3)	0	0 – 0.38
IL-15	1.91	24 (80.0)	0	0
IL-17	2.27	10 (33.3)	1.15	0 – 4.28
Eotaxin	1.23	0 (0.0)	24.96	20.25 – 27.75
FGF-β	0.6	0 (0.0)	124.02	108 – 136.92
G-CSF	1.62	4 (13.3)	13.45	5.78 – 27.77
GM-CSF	0.67	0 (0.0)	1007.91	733.85 – 1162.91
IFN-γ	1.22	7 (23.3)	10.87	0 – 19.90
IP-10	1.06	0 (0.0)	299.38	190.61 – 448.73
MCP-1	1.62	0 (0.0)	176.01	126.36 – 274.78
MIP-1α	0.06	1 (3.3)	1.00	0.66 – 1.36
MIP-1β	0.28	0 (0.0)	20.62	8.7 – 28.13
PDGF-β	0.84	7 (23.3)	3.84	0.9 – 6.18
TNF-α	1.87	1 (3.3)	9.46	4.92 – 15.32
VEGF	2.55	0 (0.0)	232.76	178.93 – 294.61
sVEGFR-1	14	0 (0.0)	122.01	84.48 – 152.99
sVEGFR-2	137	0 (0.0)	342.43	274.39 – 386.58
EGF	3.2	7 (23.3)	16.83	0 – 25.62

in 4 eyes. The presence of HRF was graded as '0' in 2 eyes, '1' in 11 eyes, '3' in 4 eyes, '4' in 3 eyes, and '5' in 5 eyes. Samples with measurable concentrations of cytokines and chemokines were included in the analysis (Table 1).

Hierarchical cluster analysis: HCA was performed to classify the patient cohort into two relatively similar groups demonstrating either 'high' or 'low' levels of cytokine expression. Figure 1 shows the heatmap representing raw data; individuals are segregated into two clusters with each cell colored in proportion to the value of standardized cytokine expression. There was no significant difference between the two cluster groups when adjusted for age and sex when each quantitative OCT parameter was assessed. At baseline, eyes in the high cytokine profile group were associated with worse BCVA, larger CMT, and greater MV. Eyes in the low cytokine profile group had better BCVA (odds ratio, OR = 0.90, [95% confidence interval (CI) 0.81–0.99], p = 0.05), indicating that with one unit worsening of BCVA, there was an average 10% reduction in odds being in the high profile group.

The low cytokine profile group also had thinner CMT (OR = 1.08, [95% CI 1.01–1.17], p = 0.03), indicating that with every 10 µm increase in CMT, there was an average 8% increase in the odds of being in the high profile group. The low cytokine profile group had better MV (OR = 2.08, [95% CI 1.10–3.90], p = 0.02); with every 1.0 mm^3 increase in MV, there was an average 108% increase in odds being in

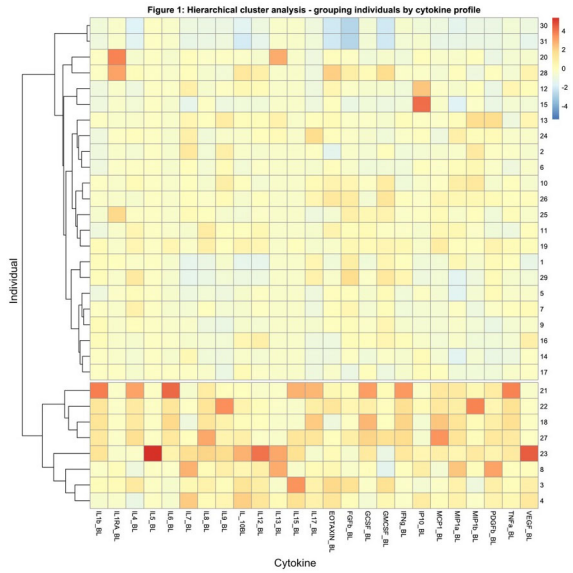

Figure 1. Heat map of hierarchical cluster analysis by clusters of low and high cytokine expression.

the high profile group. There was no significant association with SRF (OR = 1.01, [95% CI 0.99–1.02], p = 0.13). Box plots depicting the significant differences in BCVA, CMT, and MV between low and high cytokine expression profiles are shown in Figure 2.

The association between individual cytokine expression and baseline vision and OCT features: Worsened BCVA was significantly associated with increased aqueous levels of IL-7 (r = -0.45, p = 0.001), IL-9 (r = -0.41, p = 0.02), MIP-1α (r = -0.4, p = 0.03), and TNF-α (r = 0.33, p = 0.03).

With respect to quantitative OCT features, greater CMT was significantly associated with increased aqueous concentrations of IL-7 (r = 0.4, p = 0.03), IL-9 (r = 0.4, p = 0.03), and TNF-α (r = 0.39, p = 0.03). Similarly, a higher MV was also associated with increased levels of IL-7 (r = 0.37, p = 0.04), IL-9 (r = 0.39, p = 0.03), and TNF-α (r = 0.43, p = 0.02). MV was also associated with other cytokines, including IL-8 (r = 0.44, p = 0.01), IL-10 (r = 0.43, p = 0.02), IL-12 (r = 0.41, p = 0.02), IL-13 (r = 0.38, p = 0.04), IL-15 (r = 0.4, p = 0.03), MIP1α (r = 0.39, p = 0.03), and VEGF (r = 0.43, p = 0.04). The increased height of the SRF was significantly associated with raised aqueous levels of IL-15 (r = 0.40, p = 0.03) and eotaxin (r = 0.47, p = 0.008). Although Spearman's correlation may be found to be weak, such as with an r = 0.2–0.4 or moderate r = 0.4–0.6, with sufficient sample size, this correlation may be found to be statistically significant (p <0.05). The lower the p-value, the higher the likelihood of the association, whether weak, moderate, or strong. These moderate correlations suggest that the individual cytokine had an impact on the OCT parameter, but other cytokines were also involved. These correlations are shown in Table 2 and depicted in Appendix 1.

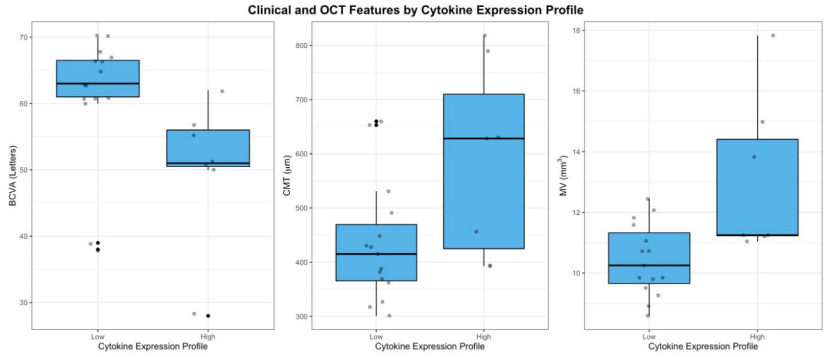

Figure 2. Boxplots of the best-corrected vision, central macular thickness, and macular volume with respect to low versus high cytokine expression profile. BCVA, best-corrected visual acuity (letters); CMT, central macular thickness (microns); MV, macular volume (mm^3).

Table 2. Spearman's rho correlation for individual cytokines associated with qualitative optical coherence tomography features in eyes with diabetic macular edema at baseline.

Cytokine	Quantitative OCT features (Spearman's rho [ρ])							
	BCVA		CMT		MV		SRF	
	rho (ρ)	P	rho (ρ)	P	rho (ρ)	P	rho (ρ)	P
IL-1β	0.013	0.94	0.18	0.35	0.24	0.20	−0.016	0.93
IL-1RA	−0.33	0.07	−0.12	0.54	0.019	0.92	−0.26	0.16
IL-4	0.12	0.54	0.018	0.92	−0.01	0.94	0.06	0.74
IL-6	−0.05	0.78	−0.11	0.58	0.23	0.22	−0.18	0.35
IL-7	**-0.45**	**0.01***	**0.40**	**0.03***	**0.37**	**0.04***	0.26	0.16
IL-8	−0.29	0.13	0.17	0.36	**0.44**	**0.01***	0.03	0.88
IL-9	**-0.41**	**0.02***	**0.40**	**0.03***	**0.39**	**0.03***	0.14	0.47
IL-10	−0.15	0.44	0.20	0.28	**0.43**	**0.01***	0.13	0.48
IL-12	−0.28	0.14	0.12	0.54	**0.41**	**0.02***	0.17	0.38
IL-13	−0.33	0.07	0.16	0.39	**0.38**	**0.04***	0.16	0.40
IL-15	−0.27	0.14	0.33	0.08	**0.40**	**0.03***	**0.40**	**0.03***
IL-17	−0.25	0.19	0.29	0.13	0.21	0.27	0.31	0.09
Eotaxin	−0.17	0.38	0.22	0.25	0.35	0.06	**0.47**	**0.008***
FGF-β	0.04	0.85	0.21	0.26	0.09	0.63	0.14	0.47
G-CSF	−0.01	0.94	0.057	0.76	0.26	0.17	−0.10	0.60
GM-CSF	0.17	0.37	0.21	0.26	0.10	0.59	0.11	0.57
IFN-γ	−0.13	0.50	0.16	0.41	0.26	0.16	−0.10	0.58
IP-10	−0.23	0.22	0.15	0.41	0.29	0.12	0.18	0.35
MCP-1	−0.21	0.26	0.21	0.28	0.24	0.21	0.02	0.63
MIP-1α	**-0.40**	**0.028***	0.23	0.21	**0.39**	**0.034***	0.18	0.35
MIP-1β	−0.32	0.08	0.34	0.07	0.26	0.16	0.11	0.57
PDGF-β	−0.21	0.26	0.20	0.30	0.30	0.11	0.05	0.78
TNF-α	**-0.39**	**0.03***	**0.39**	**0.03***	**0.43**	**0.02***	0.27	0.14
VEGF	−0.14	0.47	0.14	0.46	**0.38**	**0.04***	0.16	0.41
sVEGFR-1	−0.33	0.12	−0.05	0.84	0.05	0.83	0.01	0.96
sVEGFR-2	−0.06	0.76	−0.01	0.95	−0.16	0.46	0.37	0.09

BCVA=Best-corrected visual acuity, CMT=Central macular thickness, MV=Macular volume, SRF=Subretinal fluid height, *=Statistically significant p≤0.05

The association of aqueous cytokine concentrations and the qualitative features is shown in Table 3, with respective median and interquartile ranges shown in Appendix 2. In keeping with the association of TNF-α with worse BCVA, CMT, and MV at baseline, smaller but more numerous IRC were also found to be associated with greater levels of TNF-α (H = 8.17, p = 0.02), whereas larger IRC were more likely to be observed with lower levels of TNF-α. A similar finding was observed with IFN-γ, with higher concentrations (H = 7.39, p = 0.03) being associated with the presence of smaller and numerous IRC. FGF-β (H = 6.74, p = 0.03) and GM-CSF (H = 6.99, p = 0.03) had more variable associations, with higher concentrations being associated with intermediate size cysts with lower concentrations visible in smaller and larger IRC.

Higher aqueous concentrations of IL-6 (W = 39, p = 0.04), IL-13 (W = 44, p = 0.02), and sVEGFR-1 (W = 25.5, p = 0.05) were more likely to be observed in eyes with DRIL, while higher levels of GM-CSF (W = 131, p = 0.01) were protective. The significant associations are illustrated in Figure 3.

Table 3. Individual cytokines associated with qualitative optical coherence tomography features in eyes with diabetic macular edema at baseline.

Cytokine	Qualitative OCT features (Mann–Whitney† and Kruskal–Wallis‡)					
	IRC size‡ *H,* (p value)	Pattern‡ *H,* (p value)	HRF‡ *H,* (p value)	EZ/ELM† *W,* (p value)	DRIL† *W,* (p value)	ERM/VMT† *W,* (p value)
IL-1β	5.70, (0.06)	1.03, (0.60)	2.62, (0.27)	67.0, (0.81)	59.0, (0.30)	41.5, (0.54)
IL-1RA	1.25, (0.53)	5.59, (0.06)	3.90, (0.14)	36.0, (0.06)	54.5, (0.20)	63/0, (0.51)
IL-4	2.64, (0.27)	0.72, (0.70)	2.78, (0.25)	72.0, (1.00)	97.0, (0.43)	60.5, (0.62)
IL-6	3.40, (0.18)	1.21, (0.55)	3.53, (0.17)	75.0, (0.9)	**39.0, (0.04)***	31/0, (0.22)
IL-7	0.69, (0.71)	1.05, (0.59)	2.88, (0.24)	44.0, (0.15)	70.0, (0.62)	50.5, (0.95)
IL-8	1.41, (0.50)	0.65, (0.72)	1.00, (0.606)	73.0, (0.98)	52.0, (0.17)	39.0, (0.47)
IL-9	0.50, (0.78)	1.57, (0.46)	0.61, (0.74)	60.0, (0.56)	66.0, (0.50)	29.0, (0.18)
IL-10	1.68, (0.43)	1.00, (0.61)	2.19, (0.33)	60.5, (0.57)	52.0, (0.17)	50.0, (0.93)
IL-12	1.32, (0.52)	0.98, (0.61)	1.94, (0.38)	65.6 (0.76)	65.6, (0.48)	46.0, (0.74)
IL-13	0.40, (0.82)	2.76, (0.25)	0.18, (0.91)	48.0, (0.12)	**44.0, (0.02)***	37.5, (0.27)
IL-15	3.06, (0.22)	3.16, (0.21)	0.75, (0.69)	54.0, (0.19)	74.0, (0.67)	49.0, (0.83)
IL-17	2.80, (0.25)	2.79, (0.25)	0.02, (0.99)	64.0, (0.69)	93.5, (0.53)	41.5, (0.53)
Eotaxin	1.86, (0.40)	**7.05, (0.029)***	0.41, (0.82)	41.0, (0.11)	82.5, (0.94)	39.0, (0.45)
FGF-β	**(6.74, (0.03)***	0.61, (0.74)	3.02, (0.22)	54.0, (0.36)	114.5, (0.1)	56.0, (0.83)
GM-CSF	**6.99, (0.03)***	0.40, (0.82)	2.35, (0.31)	70.0, (0.94)	**131.0, (0.01)***	66.0, (0.43)
IFN-γ	**7.39, (0.03)***	0.42, (0.81)	0.42, (0.81)	65.0, (0.73)	69.0, (0.59)	33.0, (0.25)
IP-10	0.87, (0.65)	0.89, (0.64)	2.05, (0.36)	48.0, (0.23)	44.0, (0.08)	39.0, (0.46)

Cytokine	Qualitative OCT features (Mann–Whitney† and Kruskal–Wallis‡)					
	IRC size‡ *H,* **(p value)**	**Pattern‡** *H,* **(p value)**	**HRF‡** *H*, **(p value)**	**EZ/ELM†** *W*, **(p value)**	**DRIL†** *W*, **(p value)**	**ERM/VMT†** *W*, **(p value)**
MCP-1	3.14, (0.21)	0.63, (0.73)	1.78, (0.41)	70.0, (0.94)	69.5, (0.61)	37.0, (0.38)
MIP-1α	2.79, (0.25)	0.99, (0.61)	0.11, (0.94)	60.5, (0.57)	74.0, (0.77)	42.5, (0.58)
MIP-1β	0.93 (0.63)	1.36, (0.51)	0.54, (0.76)	66.0, (0.78)	71.0, (0.67)	32.0, (0.25)
PDGF-β	3.97, (0.14)	0.70, (0.71)	0.08, (0.96)	46.0, (0.18)	74.5, (0.79)	48.0, (0.83)
TNF-α	**8.17, (0.02)***	1.24, (0.54)	1.91, (0.39)	53.0, (0.34)	63.5, (0.42)	36.5, (0.36)
VEGF	1.76, (0.42)	1.12, (0.57)	3.39, (0.18)	70.0, (0.94)	70.5, (0.64)	46.5, (0.76)
sVEGFR-1	0.46, (0.80)	1.33, (0.52)	2.43, (0.30)	31.5, (0.33)	**25.5, (0.05)***	23.0, (0.55)
sVEGFR-2	5.62, (0.06)	3.51, (0.17)	0.23, (0.89)	51.0, (0.68)	54.5, (0.95)	43.5, (0.23)

†=Mann–Whitney Test,‡=Kruskal–Wallis Test, *=statistically significant p≤0.05. *H*=Chi-square statistic, *W*=W statistic, IRC=intraretinal cyst, HRF=hyper-reflective foci, EZ/ELM=ellipsoid zone/external limiting membrane integrity, DRIL=disruption of retinal inner layers, ERM/VMT=epiretinal membrane/vitreomacular traction. Degrees of freedom=2, for both DME Pattern and IRC (Kruskal–Wallis test). Median and Interquartile ranges are shown in Appendix 2.

Molecular Vision 2023; 29:140-152 <http://www.molvis.org/molvis/v29/140>

DISCUSSION

This study demonstrated an association of several inflammatory cytokines with quantitative features of DME, such as BCVA, CMT, MV, and SRF, and qualitative features seen on OCT. From the hierarchical cluster analysis, we found that higher concentrations of inflammation-associated cytokines were associated with worse BCVA, greater CMT, and larger MV at baseline. Specifically, we found that higher concentrations of TNF-α, IL-7, and IL-9 were associated with worse BCVA, greater CMT, and a larger MV. Similarly, higher MIP-1α concentrations were associated with greater MV and worse BCVA but not CMT. Although CMT has evolved as the most commonly used OCT measurement of DME in both research and clinical practice, features greatly affecting CMT, such as large IRC, may not accurately reflect changes in MV, generalized macular thickening, disease severity, or BCVA [30,31]. Thus, MV has been suggested as the most appropriate parameter for assessing the anatomic severity of DME. Accordingly, multiple other cytokines, including IL-8, IL-10, IL-12, IL-13, IL-15, and VEGF, were also positively associated with greater MV. Interestingly, increased aqueous VEGF concentrations were only associated with increased MV, with no correlation with BCVA or other OCT features.

Our study also demonstrated the association of several cytokines with the qualitative OCT features of DME at baseline. Smaller but more numerous intraretinal cysts were associated with greater levels of TNF-α and IFN-γ, whereas increased levels of IL-6, IL-13, and sVEGFR-1 were associated with an increased likelihood of DRIL.

Previous reports have suggested a wide range of aqueous cytokines involved in DME, with a few cytokines such as TNF-α, IL-1β, IL-6 and MCP-1 frequently associated with DME or its features [3,4,20]. However, this has not been consistent across previous studies, which demonstrate conflicting and heterogeneous results with various other cytokines often identified [6,7,32,33].

Most groups performed their analyses by examining a certain range of cytokines from ELISA or multiplex-based assays, which were then individually correlated to clinical features or outcomes [3,8-10,17,18,21,34-43]. However, with generally small numbers of subjects in these studies, it may be difficult to ascertain the involvement or contribution of individual cytokines to a wide range of OCT manifestations or treatment responses. This is because cytokines are involved in complex and unclear mechanisms in DME, where both pro- and anti-inflammatory cytokines are involved in multiple networks and cascades, with regulatory feedback mechanisms functioning in autocrine or paracrine loops [44]. Inflammatory cytokines also exhibit multiple and diverse functions, and their activity may fluctuate according to the pathological state of the disease, whether acute, chronic, worsening, or improving [45]. Thus, it would be helpful to first explore the association of DME with an overview of cytokines by clustering those concordantly expressed in higher concentrations.

The HCA analysis enabled this study to demonstrate that high cytokine expression is associated with DME severity. Performing HCA analysis enables a novel method of clustering inflammatory cytokines, BCVA, CMT, and MVT into relatively similar groups called clusters. The correlation of the high cytokine expression group with the main outcome measures of DME demonstrates the importance of the

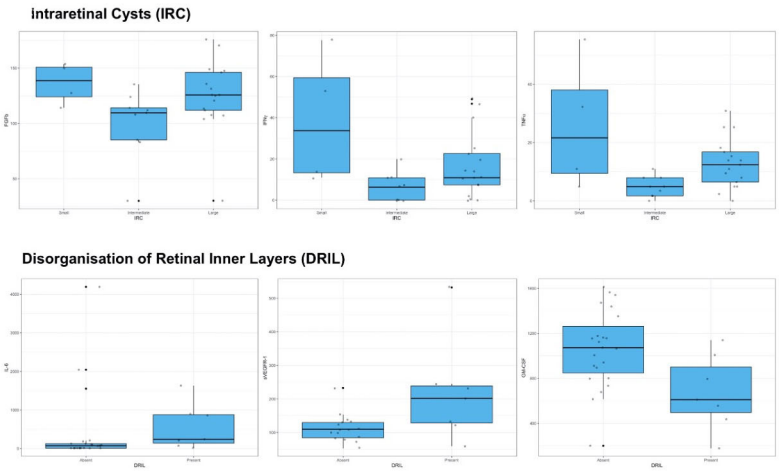

Figure 3. Plots showing the relationship of aqueous cytokine concentrations with optical coherence tomography features of eyes with diabetic macular edema at baseline.

expression of multiple inflammatory cytokines in the pathophysiological process of DME. The analysis of a large range of cytokines has enabled the identification of multiple inflammatory cytokines associated with disease severity, including IL-7 and IL-9, which have not been previously assessed in DME but have been shown to induce the secretion of TNF-α, IL-1β and IL-6 in bone marrow-derived dendritic cells [46].

TNF-α appears to be a critical element in the pathogenesis of DR. We found that increased aqueous concentrations of TNF-α were not only associated with BCVA, CMT, and MV but were also specifically associated with the presence of microcystic edema. This may relate to the presence of a more acute inflammatory phenotype of DME, as opposed to the larger IRC typically seen in the chronic structural morphology of cystoid degeneration in DME [47,48].

TNF-α is a potent inducer of VEGF, which plays a central role in promoting retinal neovascularization and vascular leakage. TNF-α mediated retinal leukostasis and apoptosis may also contribute to DME by the progressive breakdown in the blood–retina barrier and the increase in retinal endothelial cell permeability via disruption of tight junction complexes [49,50]. Treatment with intravitreal anti-VEGF agents has also been shown to reduce intraocular TNF-α levels, suggesting that the mechanisms of VEGF and inflammatory pathways involving TNF-α are intimately tied in DR [7,51]. The correlation of TNF-α to important quantitative outcome measures of DME, including BCVA, CMT, MV, and IRC, supports its prominent and central role in DME. In the clinical setting, measuring intraocular cytokines may reveal a more inflammatory process or phenotype, thus allowing clinicians to adjust their treatment accordingly.

Our study has limitations that should be acknowledged. First, aqueous sampling was used as a measure of posterior segment pathology. Analysis of vitreous fluid may be more accurate in reflecting DME severity; however, sampling is more invasive and is less preferred by our group and other researchers [3,8,20,52]. Cytokine concentrations found below the lower limit of detection were recoded as zero values and included in the statistical analysis. Although there are various methods of handling these values, with none that are particularly agreed upon [53], they may be of some importance when measuring cytokines or biomarkers in the eye, where concentrations may be relatively low. Recoding these values as zero (instead of as missing values) and including them for statistical analysis may underestimate type II statistical errors, or reduce false positives, which we conceived to be more evaluative for our exploratory analyses.

In correlating cytokines with the OCT features of DME, our study had a small sample size, limiting statistical power. Despite this, the results were statistically significant. We are reassured by the results of the HCA that high expression levels of cytokines are influenced by the main clinical parameters of DME, as assessed based on BCVA, CMT, and MV. Furthermore, multivariate regression analysis found overlap of similar cytokines significantly associated with these parameters. Lastly, analyzing a large number of cytokines raises the possibility of statistical errors related to multiple testing. Although we applied the Benjami & Hochberg method to address this, there are no agreed criteria to apply multiple testing correction methods [54], and multiple comparisons in this study need to be interpreted with caution.

In conclusion, we note that correlating individual cytokines with features of DME is difficult, given the complexity of cytokine functions within inflammatory cascades and the considerable disease overlap of imaging features. The HCA in our study demonstrated that in addition to VEGF, there is a significant contribution of inflammation-associated cytokines to the severity of DME. Specifically, TNF-α, IL-7 and IL-9, appear to be associated with OCT features of worse DME severity. Correlating imaging biomarkers of DME with inflammatory cytokines may allow clinicians to easily assess cases on OCT that portray a greater inflammatory phenotype and thus influence individualized therapeutic decision making.

APPENDIX 1. SUPPLEMENTARY FIGURE 1.

To access the data, click or select the words "Appendix 1." Scatter plots with loess curve fitted for cytokines associated with quantitative optical coherence tomography features in eyes with diabetic macular edema at baseline

APPENDIX 2. SUPPLEMENTARY TABLE 1.

To access the data, click or select the words "Appendix 2."

ACKNOWLEDGMENTS

This work was supported by a grant from Novartis Pharma AG. The Centre for Eye Research Australia receives Operational Infrastructure Support from the Victorian Government.

REFERENCES

1. Klaassen I, Van Noorden CJ, Schlingemann RO. Molecular basis of the inner blood-retinal barrier and its breakdown in diabetic macular edema and other pathological conditions. Prog Retin Eye Res 2013; 34:19-48. [PMID: 23416119].

2. Mesquida M, Drawnel F, Fauser S. The role of inflammation in diabetic eye disease. Semin Immunopathol 2019; 41:427-45. [PMID: 31175392].

3. Hillier RJ, Ojaimi E, Wong DT, Mak MY, Berger AR, Kohly RP, Kertes PJ, Forooghian F, Boyd SR, Eng K, Altomare F, Giavedoni LR, Nisenbaum R, Muni RH. Aqueous Humor Cytokine Levels as Biomarkers of Disease Severity in Diabetic Macular Edema. Retina 2017; 37:761-9. [PMID: 27471825].

4. Funatsu H, Yamashita H, Ikeda T, Mimura T, Eguchi S, Hori S. Vitreous levels of interleukin-6 and vascular endothelial growth factor are related to diabetic macular edema. Ophthalmology 2003; 110:1690-6. [PMID: 13129863].

5. Funatsu H, Yamashita H, Nakamura S, Mimura T, Eguchi S, Noma H, Hori S. Vitreous levels of pigment epithelium-derived factor and vascular endothelial growth factor are related to diabetic macular edema. Ophthalmology 2006; 113:294-301. [PMID: 16406543].

6. Wei Q, Wan Z, Hu Y, Peng Q. Cytokine and Chemokine Profile Changes in Patients After Intravitreal Conbercept Injection for Diabetic Macular Edema. Drug Des Devel Ther 2019; 13:4367-74. [PMID: 31920286].

7. Lim SW, Bandala-Sanchez E, Kolic M, Rogers SL, McAuley AK, Lim LL, Wickremasinghe SS. The Influence of Intravitreal Ranibizumab on Inflammation-associated Cytokine Concentrations in Eyes With Diabetic Macular Edema. Invest Ophthalmol Vis Sci 2018; 59:5382-90. [PMID: 30452591].

8. Shimura M, Yasuda K, Motohashi R, Kotake O, Noma H. Aqueous cytokine and growth factor levels indicate response to ranibizumab for diabetic macular oedema. Br J Ophthalmol 2017; 101:1518-23. [PMID: 28270488].

9. Felfeli T, Juncal VR, Hillier RJ, Mak MYK, Wong DT, Berger AR, Kohly RP, Kertes PJ, Eng KT, Boyd SR, Altomare F, Giavedoni LR, Muni RH. Aqueous Humor Cytokines and Long-Term Response to Anti-Vascular Endothelial Growth Factor Therapy in Diabetic Macular Edema. Am J Ophthalmol 2019; 206:176-83. [PMID: 30959004].

10. Coughlin BA, Guha-Niyogi P, Sikorskii A, Glazer LC, Mohr S. Ranibizumab Alters Levels of Intraocular Soluble Cytokine Receptors in Patients with Diabetic Macular Edema. Curr Eye Res 2020; 45:509-20. [PMID: 31488015].

11. Nguyen QD, Brown DM, Marcus DM, Boyer DS, Patel S, Feiner L, Gibson A, Sy J, Rundle AC, Hopkins JJ, Rubio RG, Ehrlich JS. Rise, Group RR. Ranibizumab for diabetic macular edema: results from 2 phase III randomized trials: RISE and RIDE. Ophthalmology 2012; 119:789-801. [PMID: 22330964].

12. Elman MJ, Ayala A, Bressler NM, Browning D, Flaxel CJ, Glassman AR, Jampol LM, Stone TW. Diabetic Retinopathy Clinical Research N. Intravitreal Ranibizumab for diabetic macular edema with prompt versus deferred laser treatment: 5-year randomized trial results. Ophthalmology 2015; 122:375-81. [PMID: 25439614].

13. Bressler NM, Beaulieu WT, Glassman AR, Blinder KJ, Bressler SB, Jampol LM, Melia M, Wells JA 3rd. Diabetic Retinopathy Clinical Research N. Persistent Macular Thickening Following Intravitreous Aflibercept, Bevacizumab, or Ranibizumab for Central-Involved Diabetic Macular Edema With Vision Impairment: A Secondary Analysis of a Randomized Clinical Trial. JAMA Ophthalmol 2018; 136:257-69. [PMID: 29392288].

14. Maturi RK, Glassman AR, Liu D, Beck RW, Bhavsar AR, Bressler NM, Jampol LM, Melia M, Punjabi OS, Salehi-Had H, Sun JK. Diabetic Retinopathy Clinical Research N. Effect of Adding Dexamethasone to Continued Ranibizumab Treatment in Patients With Persistent Diabetic Macular Edema: A DRCR Network Phase 2 Randomized Clinical Trial. JAMA Ophthalmol 2018; 136:29-38. [PMID: 29127949].

15. Iglicki M, Busch C, Zur D, Okada M, Mariussi M, Chhablani JK, Cebeci Z, Fraser-Bell S, Chaikitmongkol V, Couturier A, Giancipoli E, Lupidi M, Rodriguez-Valdes PJ, Rehak M, Fung AT, Goldstein M, Loewenstein A. DEXAMETHASONE IMPLANT FOR DIABETIC MACULAR EDEMA IN NAIVE COMPARED WITH REFRACTORY EYES: The International Retina Group Real-Life 24-Month Multicenter Study. The IRGREL-DEX Study. Retina 2019; 39:44-51. [PMID: 29697589].

16. Whitcup SM, Cidlowski JA, Csaky KG, Ambati J. Pharmacology of Corticosteroids for Diabetic Macular Edema. Invest Ophthalmol Vis Sci 2018; 59:1-12. [PMID: 29297055].

17. Sohn HJ, Han DH, Kim IT, Oh IK, Kim KH, Lee DY, Nam DH. Changes in aqueous concentrations of various cytokines after intravitreal triamcinolone versus bevacizumab for diabetic macular edema. Am J Ophthalmol 2011; 152:686-94. [PMID: 21782151].

18. Podkowinski D, Orlowski-Wimmer E, Zlabinger G, Pollreisz A, Mursch-Edlmayr AS, Mariacher S, Ring M, Bolz M. Aqueous humour cytokine changes during a loading phase of intravitreal ranibizumab or dexamethasone implant in diabetic macular oedema. Acta Ophthalmol 2020; 98:e407-15. [PMID: 31736269].

19. Panozzo G, Cicinelli MV, Augustin AJ, Battaglia Parodi M, Cunha-Vaz J, Guarnaccia G, Kodjikian L, Jampol LM, Junemann A, Lanzetta P, Lowenstein A, Midena E, Navarro R, Querques G, Ricci F, Schmidt-Erfurth U, Silva RMD, Sivaprasad S, Varano M, Virgili G, Bandello F. An optical coherence tomography-based grading of diabetic maculopathy proposed by an international expert panel: The European School for Advanced Studies in Ophthalmology classification. Eur J Ophthalmol 2020; 30:8-18. [PMID: 31718271].

20. Abraham JR, Wykoff CC, Arepalli S, Lunasco L, Yu HJ, Hu M, Reese J, Srivastava SK, Brown DM, Ehlers JP. Aqueous Cytokine Expression and Higher Order OCT Biomarkers: Assessment of the Anatomic-Biologic Bridge in the IMAGINE DME Study. Am J Ophthalmol 2021; 222:328-39. [PMID: 32896498].

21. Sonoda S, Sakamoto T, Yamashita T, Shirasawa M, Otsuka H, Sonoda Y. Retinal morphologic changes and concentrations of cytokines in eyes with diabetic macular edema. Retina 2014; 34:741-8. [PMID: 23975003].

22. Mitchell P, Bandello F, Schmidt-Erfurth U, Lang GE, Massin P, Schlingemann RO, Sutter F, Simader C, Burian G, Gerstner

O, Weichselberger A. group Rs. The RESTORE study: ranibizumab monotherapy or combined with laser versus laser monotherapy for diabetic macular edema. Ophthalmology 2011; 118:615-25. [PMID: 21459215].

23. Seo KH, Yu SY, Kim M, Kwak HW. Visual and Morphologic Outcomes of Intravitreal Ranibizumab for Diabetic Macular Edema Based on Optical Coherence Tomography Patterns. Retina 2016; 36:588-95. [PMID: 26398695].

24. Koleva-Georgieva D, Sivkova N. Assessment of serous macular detachment in eyes with diabetic macular edema by use of spectral-domain optical coherence tomography. Graefes Arch Clin Exp Ophthalmol 2009; 247:1461-9. [PMID: 19547995].

25. Panozzo G, Parolini B, Gusson E, Mercanti A, Pinackatt S, Bertoldo G, Pignatto S. Diabetic macular edema: an OCT-based classification. Semin Ophthalmol 2004; 19:13-20. [PMID: 15658007].

26. Uji A, Murakami T, Nishijima K, Akagi T, Horii T, Arakawa N, Muraoka Y, Ellabban AA, Yoshimura N. Association between hyperreflective foci in the outer retina, status of photoreceptor layer, and visual acuity in diabetic macular edema. Am J Ophthalmol. 2012;153(4):710–7, 7 e1.

27. Sun JK, Lin MM, Lammer J, Prager S, Sarangi R, Silva PS, Aiello LP. Disorganization of the retinal inner layers as a predictor of visual acuity in eyes with center-involved diabetic macular edema. JAMA Ophthalmol 2014; 132:1309-16. [PMID: 25058813].

28. Vujosevic S, Bini S, Torresin T, Berton M, Midena G, Parrozzani R, Martini F, Pucci P, Daniele AR, Cavarzeran F, Midena E. HYPERREFLECTIVE RETINAL SPOTS IN NORMAL AND DIABETIC EYES: B-Scan and En Face Spectral Domain Optical Coherence Tomography Evaluation. Retina 2017; 37:1092-103. [PMID: 27668929].

29. Duker JS, Kaiser PK, Binder S, de Smet MD, Gaudric A, Reichel E, Sadda SR, Sebag J, Spaide RF, Stalmans P. The International Vitreomacular Traction Study Group classification of vitreomacular adhesion, traction, and macular hole. Ophthalmology 2013; 120:2611-9. [PMID: 24053995].

30. Deak GG, Schmidt-Erfurth UM, Jampol LM. Correlation of Central Retinal Thickness and Visual Acuity in Diabetic Macular Edema. JAMA Ophthalmol 2018; 136:1215-6. [PMID: 30193350].

31. Gerendas BS, Prager S, Deak G, Simader C, Lammer J, Waldstein SM, Guerin T, Kundi M, Schmidt-Erfurth UM. Predictive imaging biomarkers relevant for functional and anatomical outcomes during ranibizumab therapy of diabetic macular oedema. Br J Ophthalmol 2018; 102:195-203. [PMID: 28724636].

32. Podkowinski D, Orlowski-Wimmer E, Zlabinger G, Pollreisz A, Mursch-Edlmayr AS, Mariacher S, Ring M, Bolz M. Aqueous humour cytokine changes during a loading phase of intravitreal ranibizumab or dexamethasone implant in diabetic macular oedema. Acta Ophthalmol 2020; [PMID: 31736269].

33. Song S, Yu X, Zhang P, Dai H. Increased levels of cytokines in the aqueous humor correlate with the severity of diabetic retinopathy. J Diabetes Complications 2020; 34:107641-[PMID: 32605862].

34. Hillier RJ, Ojaimi E, Wong DT, Mak MYK, Berger AR, Kohly RP, Kertes PJ, Forooghian F, Boyd SR, Eng K, Altomare F, Giavedoni LR, Nisenbaum R, Muni RH. Aqueous Humor Cytokine Levels and Anatomic Response to Intravitreal Ranibizumab in Diabetic Macular Edema. JAMA Ophthalmol 2018; 136:382-8. [PMID: 29522144].

35. Yi QY, Wang YY, Chen LS, Li WD, Shen Y, Jin Y, Yang J, Wang Y, Yuan J, Cheng L. Implication of inflammatory cytokines in the aqueous humour for management of macular diseases. Acta Ophthalmol 2020; 98:e309-15. [PMID: 31531945].

36. Abraham JR, Wykoff CC, Arepalli S, Lunasco L, Yu HJ, Hu M, Reese J, Srivastava SK, Brown DM, Ehlers JP. Aqueous Cytokine Expression and Higher-Order OCT Biomarkers: Assessment of the Anatomic-Biologic Bridge in the IMAGINE DME Study. Am J Ophthalmol 2021; [PMID: 32896498].

37. Kim M, Kim Y, Lee SJ. Comparison of aqueous concentrations of angiogenic and in fl ammatory cytokines based on optical coherence tomography patterns of diabetic macular edema. Indian J Ophthalmol 2015; 63:312-7. [PMID: 26044469].

38. Bandyopadhyay S, Bandyopadhyay SK, Saha M, Sinha A. Study of aqueous cytokines in patients with different patterns of diabetic macular edema based on optical coherence tomography. Int Ophthalmol 2018; 38:241-9. [PMID: 28160192].

39. Lee H, Jang H, Choi YA, Kim HC, Chung H. Association Between Soluble CD14 in the Aqueous Humor and Hyperreflective Foci on Optical Coherence Tomography in Patients With Diabetic Macular Edema. Invest Ophthalmol Vis Sci 2018; 59:715-21. [PMID: 29392317].

40. Sabaner MC, Akdogan M, Dogan M, Oral AY, Duman R, Koca T, Bozkurt E. Inflammatory cytokines, oxidative and antioxidative stress levels in patients with diabetic macular edema and hyperreflective spots. Eur J Ophthalmol 2021; 31:2535-45. [PMID: 33008266].

41. Yenihayat F, Ozkan B, Kasap M, Karabas VL, Guzel N, Akpinar G, Pirhan D. Vitreous IL-8 and VEGF levels in diabetic macular edema with or without subretinal fluid. Int Ophthalmol 2019; 39:821-8. [PMID: 29524030].

42. Cacciamani A, Esposito G, Scarinci F, Parravano M, Dinice L, Di Nicola M, Micera A. Inflammatory mediators in the vitreal reflux of patients with diabetic macular edema. Graefes Arch Clin Exp Ophthalmol 2019; 257:187-97. [PMID: 30377797].

43. Hwang HB, Jee D, Kwon JW. Characteristics of diabetic macular edema patients with serous retinal detachment. Medicine (Baltimore) 2019; 98:e18333-[PMID: 31860985].

44. Nguyen QD, Tatlipinar S, Shah SM, Haller JA, Quinlan E, Sung J, Zimmer-Galler I, Do DV, Campochiaro PA. Vascular endothelial growth factor is a critical stimulus for diabetic

macular edema. Am J Ophthalmol 2006; 142:961-9. [PMID: 17046701].

45. Kinuthia UM, Wolf A, Langmann T. Microglia and Inflammatory Responses in Diabetic Retinopathy. Front Immunol 2020; 11:564077-[PMID: 33240260].

46. Li J, Chen S, Xiao X, Zhao Y, Ding W, Li XC. IL-9 and Th9 cells in health and diseases-From tolerance to immunopathology. Cytokine Growth Factor Rev 2017; 37:47-55. [PMID: 28739029].

47. Yalcin G, Ozdek S, Baran Aksakal FN. Defining Cystoid Macular Degeneration in Diabetic Macular Edema: An OCT-Based Single-center Study. Turk J Ophthalmol. 2019; 49:315-22. [PMID: 31893586].

48. Otani T, Kishi S, Maruyama Y. Patterns of diabetic macular edema with optical coherence tomography. Am J Ophthalmol 1999; 127:688-93. [PMID: 10372879].

49. Aveleira CA, Lin CM, Abcouwer SF, Ambrosio AF, Antonetti DA. TNF-alpha signals through PKCzeta/NF-kappaB to alter the tight junction complex and increase retinal endothelial cell permeability. Diabetes 2010; 59:2872-82. [PMID: 20693346].

50. van der Wijk AE, Vogels IMC, van Noorden CJF, Klaassen I, Schlingemann RO. TNFalpha-Induced Disruption of the Blood-Retinal Barrier In Vitro Is Regulated by Intracellular 3′,5′-Cyclic Adenosine Monophosphate Levels. Invest Ophthalmol Vis Sci 2017; 58:3496-505. [PMID: 28715583].

51. Xia JP, Liu SQ, Wang S. Intravitreal conbercept improves outcome of proliferative diabetic retinopathy through inhibiting inflammation and oxidative stress. Life Sci 2021; 265:118795-[PMID: 33227274].

52. Shiraya T, Kato S, Araki F, Ueta T. Effect of intravitreal ranibizumab injection on aqueous humour cytokine levels in patients with diabetic macular oedema. Acta Ophthalmol 2017; 95:e340-1. [PMID: 27545866].

53. Pfister IB, Zandi S, Gerhardt C, Spindler J, Reichen N, Garweg JG. Risks and Challenges in Interpreting Simultaneous Analyses of Multiple Cytokines. Transl Vis Sci Technol 2020; 9:27-[PMID: 32832233].

54. Stacey AW, Pouly S, Czyz CN. An analysis of the use of multiple comparison corrections in ophthalmology research. Invest Ophthalmol Vis Sci 2012; 53:1830-4. [PMID: 22408004].

Articles are provided courtesy of Emory University and the Zhongshan Ophthalmic Center, Sun Yat-sen University, P.R. China. The print version of this article was created on 17 August 2023. This reflects all typographical corrections and errata to the article through that date. Details of any changes may be found in the online version of the article.